DOI: 10.1002/ejic.200600649

Neutral, Radical [CpNi(dithiolene)] Complexes with Flexible, Nonplanar Seven-Membered Rings: [CpNi{$S_2C_2S_2(CH_2)_2X$}] (X = CH_2, CF_2, C=CH_2, S, C=O)

Mitsushiro Nomura,[a] Michel Geoffroy,[b] Prashant Adkine,[b] and Marc Fourmigué*[a]

Keywords: Nickel / S ligands / Radicals / Metallacycles / Magnetic properties

Neutral, radical [CpNi(dithiolene)] complexes fused with seven-membered rings, formulated as [CpNi{$S_2C_2S_2(CH_2)_2$-X}] (X = CH_2, CF_2, C=CH_2, S), have been synthesized in 30–60 % yields from the reactions of nickelocene with the corresponding neutral, square-planar, (dithiolene)nickel complexes [Ni{$S_2C_2S_2(CH_2)_2X$}$_2$]. [CpNi{$S_2C_2S_2(CH_2)_2X$}] (X = C=O) was prepared from nickelocene and [1,3]dithiolo[4,5-*b*][1,4]dithiepine-2,6-dione under thermal or photochemical conditions. All complexes exhibit reversible oxidation and reduction waves to the cation and anion form, respectively. The terminal groups (X) in the seven-membered ring shift their redox potentials to anodic potentials in the following order: CF_2 > C=O > S > C=CH_2 > CH_2. The singlet EPR responses of [CpNi{$S_2C_2S_2(CH_2)_2$(X)}] appear at $g \approx 2.0514$–2.0529 in dichloromethane solution at room temperature. An NIR absorption is observed at $\lambda_{max} \approx 798$–$848$ nm ($\varepsilon \approx 1700$–2400 M^{-1} cm^{-1}) in dichloromethane solution. The X-ray structures of the five complexes show two-legged piano-stool geometries around the central nickel atom (formally Ni^{III}) and strong distortions from planarity of the seven-membered $C_2S_2(CH_2)_2X$ rings. In the solid state, those radical (S = 1/2) species adopt either one-dimensional alternating chain-like motifs (X = CH_2, C=CH_2, S) or dimeric entities characterized by a singlet–triplet magnetic behavior (X = CF_2, C=O).

Introduction

(Dithiolene)nickel complexes are currently being extensively investigated from the viewpoint of optical,[1] magnetic,[2] and conductivity studies.[3] Most of these studies involve square-planar bis(dithiolene) complexes,[4] although several mono(dithiolene)nickel complexes formulated as [Ni(dithiolene)L_2] have been described where L is an imine or a phosphane.[5] Heteroleptic complexes involving dithiolene and η^5-cyclopentadienido (Cp) ligands are also known with various Cp/dithiolene ratios and different metal centers.[6] Among them, different series of paramagnetic complexes such as the d^1 cation [Cp_2Mo(dithiolene)]$^+$ have shown a wide variety of magnetic behaviors, ranging from uniform spin chains to spin ladders or antiferromagnetic ground states.[7] In this respect, the half-metallocene (dithiolene)nickel complexes formulated as [CpNi(dithiolene)] are particularly attractive since they are neutral radical (S = 1/2) species. We have recently investigated the synthesis and electronic properties of a variety of such [CpNi(dithiolene)] complexes, which are characterized by very attractive features such as a strong NIR absorption or a highly delocalized spin density.[8] Among them, [CpNi($S_2C_2R_2$)] complexes bearing simple substituents (R = CN, COOMe, CF_3, Ph, and Me) have been synthesized by several dithiolene transfer reactions from the square-planar nickel complex [Ni($S_2C_2R_2$)$_2$] to [Cp_2Ni].[8b] Complexes involving 1,2-dithiolato ligands fused with five-membered rings, such as [CpNi(dmit)],[9] [CpNi(dmid)], and [CpNi(dsit)] (dmit = 1,3-dithiol-2-thione-4,5-dithiolato; dmid = 1,3-dithiol-2-one-4,5-dithiolato; dsit = 1,3-dithiol-2-thione-4,5-diselenolato) exhibit a set of three-dimensional intermolecular interactions in the solid state that stabilize an ordered 3D antiferromagnetic ground state.[8a]

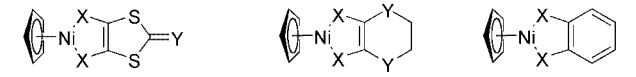

We also recently reported the CpNi(dithiolene) and -(diselenolene) complexes fused with a six-membered ring such as benzene, 5,6-dihydro-1,4-dithiine, or 5,6-dihydro-1,4-diselenine rings, as in [CpNi(dddt)], [CpNi(dsdt)], [CpNi(ddds)], [CpNi(bdt)], and [CpNi(bds)] (dddt = 5,6-dihydro-1,4-dithiine-2,3-dithiolato; ddds = 5,6-dihydro-1,4-dithiine-2,3-diselenolato; dsdt = 5,6-dihydro-1,4-diselenine-2,3-dithiolato; bdt = 1,2-benzenedithiolato; bds = 1,2-benzenediselenolato).[8c] Efficient synthetic methods were developed, and structural and magnetic investigation revealed, besides the recurrent dithiolene/dithiolene interactions, an original antiferromagnetic interaction mediated by

[a] Sciences Chimiques de Rennes, UMR 6226 CNRS – Université Rennes,
1, Campus de Beaulieu, 35042 Rennes cedex, France
Fax: +33-2-2323-6732
E-mail: marc.fourmigue@univ-rennes1.fr
[b] Department of Physical Chemistry, University of Geneva, 30 Quai Ernest Ansermet, 1211 Geneva, Switzerland

Cp···Cp overlap. We wanted to further develop these attractive series by also investigating *nonplanar* dithiolate ligands as the added flexibility in the dithiolene ligand could provide novel association patterns in the solid state for such neutral radical complexes. We report here the synthesis and electronic, structural, and magnetic properties of five paramagnetic complexes formulated as [CpNi{$S_2C_2S_2(CH_2)_2X$}] (X = CH_2, CF_2, C=CH_2, S, and C=O).

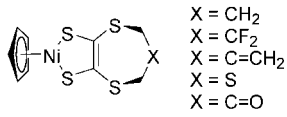

Square-planar bis(dithiolene)nickel complexes have been described with such dithiolato ligands fused with a $C_2S_2(CH_2)_2X$ seven-membered motif, all of which exhibit strong distortions from planarity, as reported for X = CH_2,[10] CF_2,[11] C=CH_2,[12] and S.[13] We wanted to investigate how those distortions might modify the electronic absorptions, crystal structures, and solid-state properties of the radical [CpNi(dithiolene)] complexes. Within this series, the dithiolato ligands where X = CF_2 and S can be considered as isosteric, as are those where X = C=CH_2 and C=O. It is therefore interesting to compare their solid-state structures to evaluate the precise role played by every X moiety in the definition of the pertinent intermolecular interactions that control their organization in the solid state. We report here the syntheses, structures, and properties of these novel complexes, which will be referred to as follows according to the nature of X: [CpNi(CH_2)], [CpNi(CF_2)], [CpNi(C=CH_2)], [CpNi(S)] and [CpNi(C=O)].

Results and Discussion

Syntheses and Molecular Properties

Faulmann et al. have reported the serendipitous formation of [CpNi(dmit)] from the reaction of [Cp_2Ni](BF_4) with Na[Ni(dmit)$_2$].[9] We have found that this complex can also be obtained in good yields from the reaction of neutral [Cp_2Ni] with the neutral square-planar nickel complexes [Ni(dithiolene)$_2$]^0.[8] Accordingly, the reaction of [Cp_2Ni] with [Ni(CH_2)$_2$]^0, [Ni(CF_2)$_2$]^0, [Ni(C=CH_2)$_2$]^0, and [Ni(S_2)]^0 at 80 °C affords the corresponding [CpNi(dithiolene)] complexes in good to fair yields: [CpNi(CH_2)] (54%), [CpNi(CF_2)] (41%), [CpNi(C=CH_2)] (30%), and [CpNi(S)] (61%) (see Scheme 1 and Entries 1–4 in Table 1).

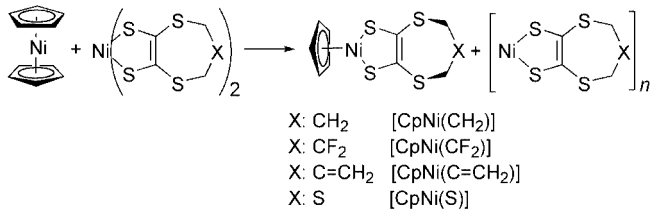

Scheme 1.

The corresponding square-planar dithiolene complex [Ni(C=O)$_2$]^0 could not be prepared in a similar manner because of the complete insolubility of the anionic precursor (Bu_4N)[Ni(C=O)$_2$], which also does not react directly with [Cp_2Ni](BF_4) (Faulmann method) for the same reason (Entry 5). We therefore envisioned alternative routes involving thermal or photochemical reactions starting from the corresponding 1,3-dithiol-2-one derivative [1,3]dithiolo-[4,5-*b*][1,4]dithiepine-2,6-dione (**1**) (Scheme 2). Its reaction with [Cp_2Ni] at 110 °C or whilst being irradiated for 24 h indeed afforded [CpNi(C=O)], but only in 9% yield. King has also reported the synthesis of [CpNi(tfd)] [tfd = bis-(trifluoromethyl)-1,2-ethenedithiolate] from the reaction of [CpNi(CO)]$_2$ with bis(trifluoromethyl)-1,2-dithiete [$S_2C_2(CF_3)_2$].[14] Accordingly, we performed the reaction of the 1,3-dithiol-2-one **1** with 0.5 equiv. of [CpNi(CO)]$_2$ at 110 °C for 6 h to obtain [CpNi(C=O)] in a slightly improved yield of 15%. Note that 1,2-dithioketones have been postulated as plausible intermediates in these thermal and photochemical reactions of 1,3-dithiol-2-ones.[15] All five complexes are air-stable compounds that are soluble in typical organic solvents (dichloromethane, toluene, acetone, and thf). Their solubility decreases upon addition of *n*-hexane.

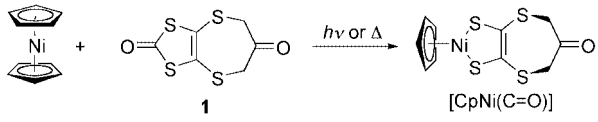

Scheme 2.

Table 1. Syntheses of CpNi(dithiolene) complexes.

Entry	Dithiolene source	CpNi source	Molar ratio	Solvent	Temperature	Time [h]	Product	Yield [%][a]
1	[Ni(CH_2)$_2$]	[Cp_2Ni]	1:1	toluene	80 °C	2	[CpNi(CH_2)]	54
2	[Ni(CF_2)$_2$]	[Cp_2Ni]	1:1	toluene	80 °C	2	[CpNi(CF_2)]	41
3	[Ni(C=CH_2)$_2$]	[Cp_2Ni]	1:1	toluene	80 °C	2	[CpNi(C=CH_2)]	30
4	[Ni(S_2)]	[Cp_2Ni]	1:1	toluene	80 °C	2	[CpNi(S)]	61
5	[Ni(C=O)$_2$]$^{-}$[b]	[Cp_2Ni](BF_4)	1:1	MeOH	reflux	2	–[c]	0
6	**1**	[Cp_2Ni]	1:1	toluene	reflux	24	[CpNi(C=O)]	9
7	**1**	[Cp_2Ni]	1:1	toluene	*hν*	24	[CpNi(C=O)]	9
8	**1**	[CpNi(CO)]$_2$	2:1	toluene	reflux	6	[CpNi(C=O)]	15

[a] Yield of isolated product. [b] As Bu_4N^+ salt. [c] No reaction.

In the reaction shown in Scheme 1, some mono(dithiolene)nickel oligomers, formulated as $[Ni\{S_2C_2S_2(CH_2)_2(X)\}]_n$ (X = CH_2, CF_2), were obtained as by-products (4–5% yields). The by-products were identified as hexamers (n = 6) by TOF mass spectrometry.[16] The other oligomers (X = C=CH_2, S) could not be isolated by column chromatography as their solubility is too low. We consider that this dithiolene transfer reaction using [Ni(dithiolene)$_2$] is different from that using $(R_4N)_2$[Zn(dithiolene)$_2$].[17] Although the Zn complex can provide both dithiolene ligands, the Ni complex can release only one of two dithiolene ligands and the remaining [Ni(dithiolene)] moiety then oligomerizes.

Characteristic cyclic voltammograms (CVs) of the [CpNi(dithiolene)] complexes $[CpNi\{S_2C_2S_2(CH_2)_2X\}]$ are shown in Figure 1, and the redox potentials of the five complexes (vs. Fc/Fc^+), together with their ΔE and ΔE_p values, are collected in Table 2. The CVs show reversible, well-defined oxidation and reduction waves.

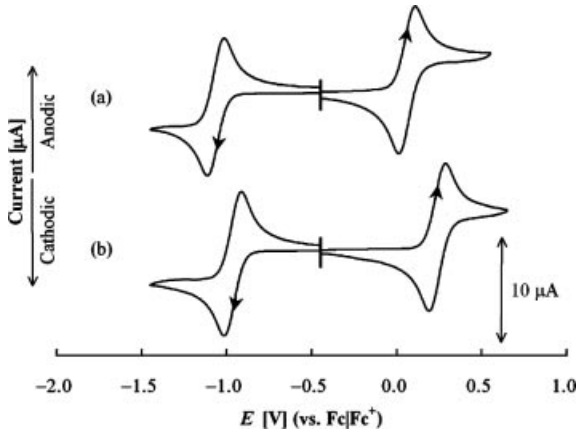

Figure 1. Cyclic voltammograms of (a) [CpNi(CH_2)] and (b) [CpNi(CF_2)] (v = 100 mV s^{-1}, working electrode 1.6 mm in diameter, Pt disk) in dichloromethane solution containing Bu_4NPF_6 (0.1 M).

The nature of the terminal X group in the seven-membered ring shifts their redox potentials to anodic potentials in the following order: CF_2 > C=O > S > C=CH_2 > CH_2. A similar tendency is also found for the redox potentials [$E_{1/2}$(–2/–1) and $E_{1/2}$(–1/0)] of the corresponding square-planar nickel complexes $[Ni\{S_2C_2S_2(CH_2)_2(X)\}_2]^n$ (n = –2, –1, 0).

The EPR spectra of the five complexes were measured in dichloromethane solution at room temperature. Singlet signals were found for [CpNi(CH_2)] (g = 2.0514), [CpNi(CF_2)] (g = 2.0529), [CpNi(C=CH_2)] (g = 2.0518), [CpNi(S)] (g = 2.0524), and [CpNi(C=O)] (g = 2.0525). These g values are almost identical to those of the other CpNi(dithiolene) complexes (g = 2.041–2.054),[8] and are smaller then those of the CpNi(diselenolene) complexes (g = 2.088–2.095).[8c] Note also that the g values of the isoelectronic (17-electron) cobalt complexes $[CpCo(tfd)]^-$ (g = 2.454)[18] and $[CpCo(mnt)]^-$ ($g \approx 2.5$)[19] are larger, thus demonstrating that the 17-electron Co(dithiolene) complexes have a large spin contribution on the metal center (formal Co^{II}), while the spin density of the nickel complex is largely delocalized on the ligands.[8]

The UV/Vis/NIR absorption spectra (Figure 2) exhibit a characteristic NIR absorption centered at ca. 800–850 nm. Their maximum absorption wavelengths (λ_{max}) and molar absorption coefficients (ε) are summarized in Table 3. Interestingly, the λ_{max} evolution with the nature of X follows the electrochemical series identified above, with the lowest energy absorption observed with the most electron-rich dithiolato ligands.

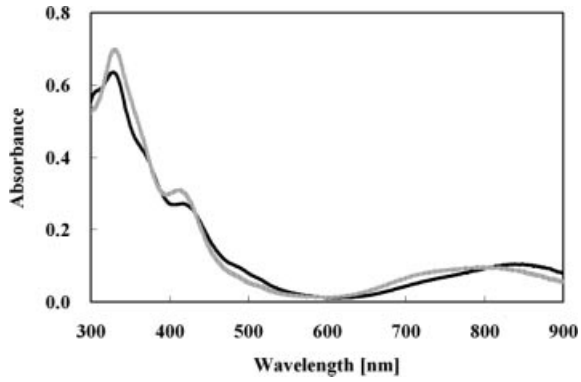

Figure 2. UV/Vis/NIR spectra of [CpNi(CH_2)] (black line) and [CpNi(CF_2)] (grey line) in dichloromethane solution (c = 5×10^{-5} M).

Table 2. Redox potentials (vs. Fc/Fc^+) of CpNi(dithiolene) complexes.

	$E_{1/2}$ (red) [V][a]	ΔE [mV]	ΔE_p [mV]	$E_{1/2}$ (ox) [V]	ΔE [mV]	ΔE_p [mV]	Ref.
[CpNi(dddt)]	–1.06	72	106	–0.02	74	106	[8c]
[CpNi(CH_2)]	–1.08	70	100	+0.07	68	92	this work
[CpNi(C=CH_2)]	–1.05	72	100	+0.12	72	100	this work
[CpNi(S)]	–1.02	70	98	+0.19	72	98	this work
[CpNi(C=O)]	–0.98	68	104	+0.22	68	98	this work
[CpNi(CF_2)]	–0.98	72	102	+0.25	72	98	this work
[CpNi(bdt)]	–1.00	68	92	+0.30	72	88	[8c]
[CpNi(dmit)]	–0.72	_[b]	100	+0.28	_[b]	100	[8c]
[CpNi(mnt)]	–0.64	_[b]	_[b]	+0.79[c]	_[b]	_[b]	[8b]

[a] $E_{1/2} = (E_p + E_{p/2})/2$, $\Delta E = |E_p - E_{p/2}|$, $\Delta E_p = |E_{pa} - E_{pc}|$. [b] Not available. [c] Irreversible.

Table 3. UV/Vis/NIR data of CpNi(dithiolene) complexes and reference compounds.

	λ_{max} [nm]	ε [$M^{-1}cm^{-1}$]	Ref.
[CpNi(dddt)]	1012	4700	[8c]
[CpNi(dmit)]	967	6000	[8c]
[CpNi(dsit)]	948	3200	[8c]
[CpNi($S_2C_2Ph_2$)]	846	2900	[8b]
[CpNi($S_2C_2Me_2$)]	835	2600	[8b]
[CpNi(CH_2)]	848	2100	this work
[CpNi($C{=}CH_2$)]	840	2400	this work
[CpNi(S)]	823	1800	this work
[CpNi(C=O)]	806	1700	this work
[CpNi(CF_2)]	798	2000	this work
[CpNi(bdt)]	722	2600	[8c]
[CpNi(mnt)]	698	2000	[8b]
[CpNi{$S_2C_2(CO_2Me)_2$}]	695	1500	[8b]

Solid-State Structural and Magnetic Properties

X-ray structure determinations were performed for the five new CpNi(dithiolene) complexes, which are not isostructural despite their closely related molecular structures: [CpNi(CH_2)] (triclinic, $P\bar{1}$), [CpNi(CF_2)] (orthorhombic, *Pbca*), [CpNi($C{=}CH_2$)] (monoclinic, $P2_1$), [CpNi(S)] (monoclinic, $P2_1/c$), and [CpNi(C=O)] (monoclinic, $P2_1/n$). The ORTEP drawings are shown in Figures 3 and 4.

Selected bond lengths and bond angles are summarized in Tables 4 and 5, respectively. The Ni–S bond lengths are ca. 2.12 Å and are therefore similar to those of the other CpNi(dithiolene) complexes (Table 4) but slightly shorter than in monoanionic square-planar bis(dithiolene) complexes such as $[Ni(CH_2)_2]^-$,[10a] $[Ni(CF_2)_2]^-$,[11a] $[Ni(C{=}CH_2)_2]^-$,[12a] and $[Ni(S)_2]^-$[13] (ca. 2.14 Å). Similarly, we observe that the C–S and C=C distances are slightly shorter and slightly longer, respectively, in the [CpNi(dithiolene)] complexes than in the anionic Ni(dithiolene)$_2^-$ complexes. Since both types of complexes are formally Ni^{III} d^7 species, the evolution of the bond lengths within the dithiolato ligand gives an indication of its contribution to the SOMO (singly occupied molecular orbital) of the complexes. Indeed, the two-electron oxidation of the dithiolato ligand leads to the corresponding dithioketone species, thus implying that partial oxidation of this ligand results in a shortening of the C–S bonds and associated lengthening of the C=C bond of the metallacycle. The fact that these trends are more marked in the [CpNi(dithiolene)] com-

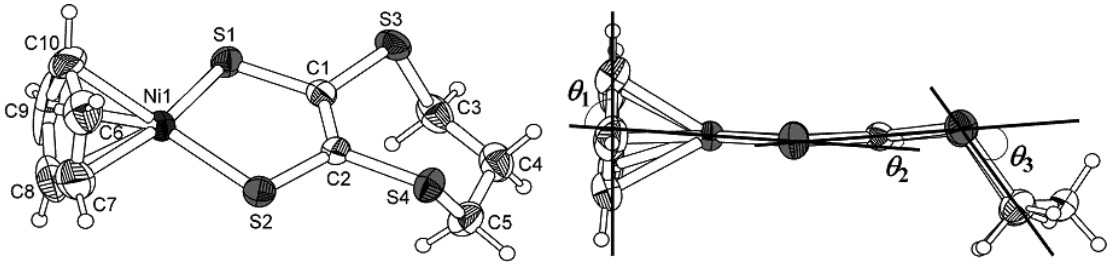

Figure 3. Left: ORTEP drawing of [CpNi(CH_2)], thermal ellipsoids are drawn at 50% probability level. Right: a side view showing the definition of the three folding angles reported in Table 6; θ_1 is the dihedral angle [°] between the Cp and NiS_2 mean planes, θ_2 represents the small folding of the metallacycle along the S···S hinge, and θ_3 the large folding of the seven-membered ring along the S···S hinge.

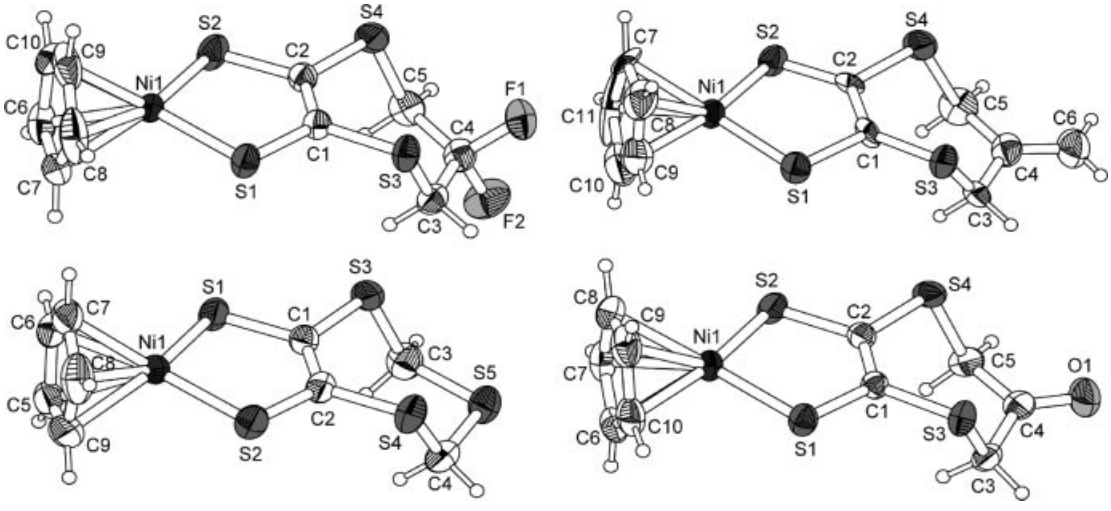

Figure 4. ORTEP drawings of [CpNi(CF_2)] (top left), [CpNi($C{=}CH_2$)] (top right), [CpNi(S)] (bottom left) and [CpNi(C=O)] (bottom right). Thermal ellipsoids are drawn at the 50% probability level.

Table 4. Selected bond lengths [Å] of CpNi(dithiolene) and square-planar Ni(dithiolene)$_2$ complexes.

	Ni1–S1	Ni1–S2	S1–C1	S2–C2	C1–C2	Ref.
[CpNi(CH_2)]	2.1242(10)	2.1242(10)	1.725(3)	1.726(3)	1.358(5)	this work
(NEt_4)[Ni(CH_2)$_2$]	2.141(1)	2.145(1)	1.728(2)	1.729(2)	1.351(3)	[10a]
[CpNi(CF_2)]	2.1195(9)	2.1314(9)	1.724(3)	1.725(3)	1.349(4)	this work
(NBu_4)[Ni(CF_2)$_2$]	2.1450(10)	2.1494(11)	1.734(4)	1.741(4)	1.338(5)	[11a]
[CpNi(C=CH_2)]	2.128(4)	2.129(4)	1.807(11)	1.636(10)	1.387(6)	this work
(NBu_4)[Ni(C=CH_2)$_2$]	2.143(2)	2.130(2)	1.726(7)	1.729(7)	1.356(8)	[12a]
[CpNi(S)]	2.1209(7)	2.1337(8)	1.729(3)	1.733(3)	1.356(4)	this work
(NBu_4)[Ni(S)$_2$]	2.141	2.139	1.716	1.712	1.377	[13]
[CpNi(C=O)]	2.1244(9)	2.1258(9)	1.729(3)	1.732(3)	1.357(4)	this work
[CpNi(dddt)]	2.125(2)	2.127(2)	1.711(10)	1.744(9)	1.336(13)	[8c]
[CpNi(bdt)]	2.1205(13)	2.1280(13)	1.731(5)	1.740(4)	1.410(6)	[8c]
[CpNi(dmit)]	2.138(2)	2.133(2)	1.706(8)	1.716(7)	1.36(1)	[9]
[CpNi(mnt)]	2.1255(8)	2.1282(8)	1.715(3)	1.725(3)	1.354(4)	[8b]

Table 5. Selected bond angles and dihedral angles [°] of CpNi(dithiolene) complexes.

	S1–Ni1–S2	Ni–S1–C1	Ni1–S2–C2	θ_1	θ_2	θ_3	Ref.
[CpNi(CH_2)]	92.42(4)	103.97(11)	103.85(11)	89.3	7.7	61.32	this work
[CpNi(CF_2)]	92.58(3)	103.78(10)	103.45(10)	89.8	5.0	66.77	this work
[CpNi(C=CH_2)]	92.51(4)	104.4(4)	103.4(3)	89.8	7.5	63.65	this work
[CpNi(S)]	92.74(3)	103.77(10)	103.67(10)	87.3	5.1	63.09	this work
[CpNi(C=O)]	93.03(3)	103.42(10)	103.64(11)	86.2	2.4	64.48	this work
[CpNi(dddt)]	92.42(9)	103.4(3)	103.7(3)	86.9	1.0, 4.3	–	[8c]
[CpNi(bdt)]	93.93(5)	103.71(15)	103.61(15)	84.9	2.7, 5.0	–	[8c]
[CpNi(dmit)]	94.97(8)	100.8(3)	100.9(3)	86.5	4.0	–	[9]
[CpNi(mnt)]	94.61(3)	101.7(1)	101.7(1)	89.9	1.4	–	[8b]

plexes than in the corresponding square-planar bis(dithiolene) ones clearly indicates a stronger participation of the dithiolato ligand in the SOMO.

These complexes adopt typical two-legged piano-stool geometries. The dihedral angle θ_1 between the Cp and NiS_2 mean planes (see Figure 3) is close to 90°, a geometry comparable to that of 16-electron $CpCo^{III}$,[20] $CpRh^{III}$,[21] $CpIr^{III}$,[22] and (η^6-arene)Ru^{II}[23] dithiolene complexes. The NiS_2C_2 metallacycle is not perfectly planar but is slightly folded along the S···S hinge with θ_2 values of between 2 and 8°, as is also observed with the complexes with dithiolato ligands fused with rigid five- (dmit, dmid) or six-membered (dddt, bdt) rings.[8] Furthermore, the dihedral angles (θ_3 in Figure 3) between the C1–C2–S3–S4 and S3–S4–C3–C5 mean planes are found in the range 61–67° (Table 5).

The solid-state organization of the complexes differs strongly from one to the other. Considering that these molecules are radicals (S = 1/2), with the spin density largely delocalized on the nickel atom, the dithiolene ligand, and the cyclopentadienido ring,[8c] their crystal structure can be analyzed in the light of possible paths for direct exchange magnetic interactions based on short contacts between the sulfur atoms of the dithiolene ligands and eventually between the Cp rings. Applying this procedure to the parent [CpNi(CH_2)] complex first reveals (Figure 5) that the only short intermolecular contact involves the sulfur atoms of the metallacycles, affording chains running along the *c*-axis with two similar S···S intermolecular distances of 3.80 and 3.83 Å.

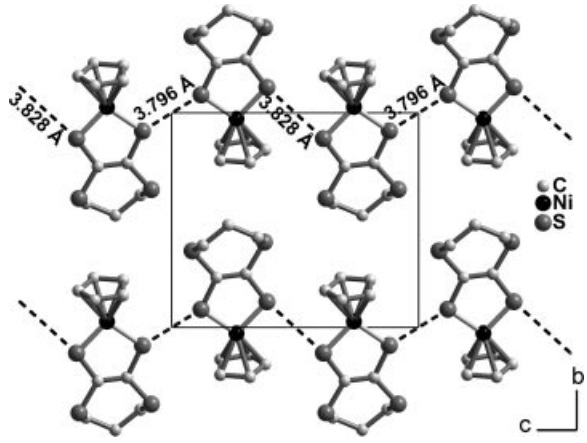

Figure 5. Projection view of the unit cell of [CpNi(CH_2)] along the *a*-axis showing the chain motif.

As shown in Figure 6, a similar chain motif is also identified in [CpNi(C=CH_2)], which gives rise, for symmetry reasons, to a uniform chain structure with equivalent S···S distances of a slightly shorter 3.75 Å.

On the other hand, a projection view of [CpNi(S)] along the *b*-axis of the structure (Figure 7) does not reveal any short intermolecular contacts; the metallacycles are almost perpendicular to each other and the shortest S···S intermolecular distance of 4.0 Å involves the sulfur atom of the thioether moiety. All other S···S contacts exceed 4.5 Å.

However, looking at the stacking of the radical complexes in the perpendicular direction (along the monoclinic

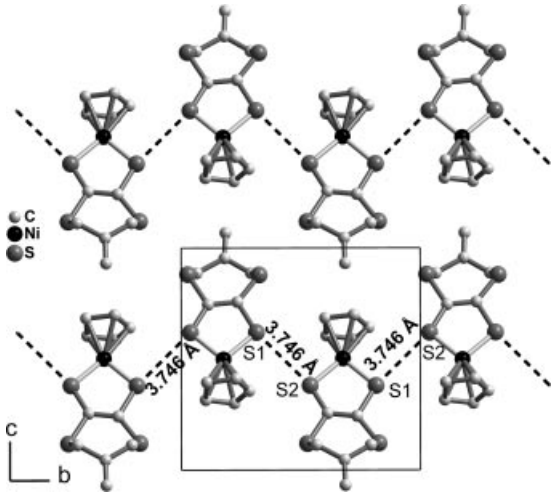

Figure 6. Projection of the unit cell of [CpNi(C=CH_2)] along the *a*-axis showing the uniform chain motif running along the *b*-axis.

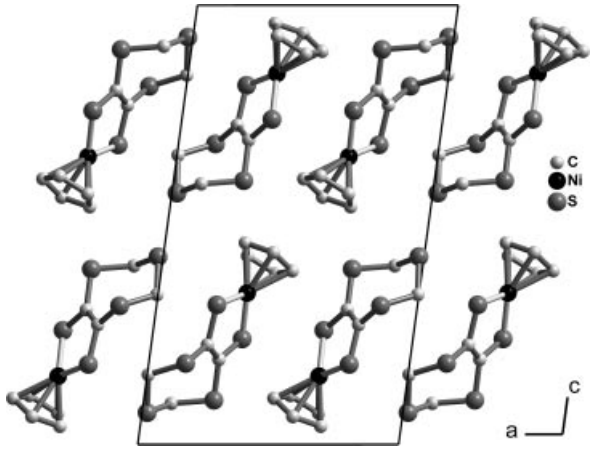

Figure 7. Projection view of [CpNi(S)] along the *b*-axis.

b-axis, Figure 8), the complexes form uniform chains that are characterized by a set on S···S intermolecular distances of between 3.69 and 4.06 Å that involve not only the sulfur atoms of the metallacycle, as already observed above in [CpNi(CH_2)] and [CpNi(C=CH_2)], but also the outer sulfur atoms of the seven-membered metallacycle.

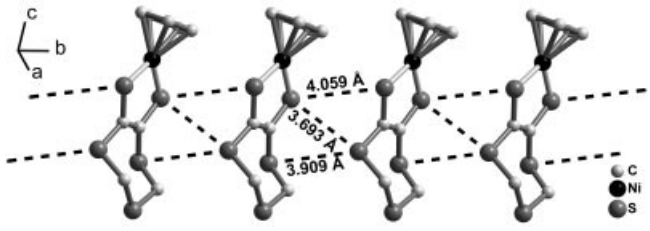

Figure 8. View of the chain-like structure of [CpNi(S)].

It is therefore expected from this structural analysis that [CpNi(S)] most probably experiences weaker antiferromagnetic interactions than the other two derivatives, as indeed observed from the temperature dependence of their magnetic susceptibility. As shown in Figure 9, all three exhibit a smooth maximum at low temperatures, characteristic of a Bonner–Fischer-type behavior of a Heisenberg uniform chain.[24] The molar susceptibility can be properly fitted in the whole temperature range (2–300 K) to the expression $\chi = \chi_0 + (1 - \rho)\cdot 0.375/T + \rho\cdot\chi_{BF}$, where χ_0 is a temperature-independent value, $(1 - \rho)\cdot 0.375/T$ (χ_C) represents a contribution of paramagnetic defaults (Curie tail), and $\rho\cdot\chi_{BF}$ is the contribution of the uniform chain; this also takes into account the *g* value of the different complexes determined from the solution EPR measurements (see above). *J*/*k* values of –39.2(3), –21.4(1), and –6.3(1) K, that is 27.2, 14.8, and 4.4 cm^{-1}, were found for [CpNi(CH_2)], [CpNi(C=CH_2)], and [CpNi(S)], respectively, with Curie tail contributions not exceeding 0.4% of $S = 1/2$ species. Note that for [CpNi(CH_2)] the chain is not really uniform from a structural point of view (Figure 5). However, attempts to use an alternating chain model to fit the data, even with a weak alternation, were unsuccessful.

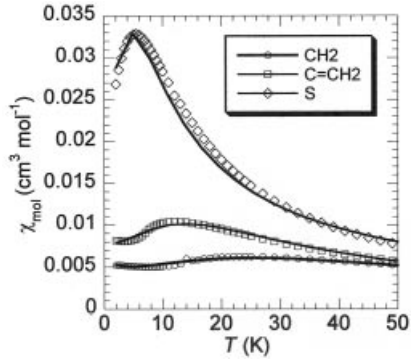

Figure 9. Temperature dependence of the magnetic susceptibility in [CpNi(CH_2)], [CpNi(C=CH_2)], and [CpNi(S)]. Solid lines are fits to the uniform spin-chain model (see text).

The situation is completely different in the two other complexes, thereby illustrating the flexibility and adaptability of these series. As shown in Figure 10, [CpNi(CF_2)] molecules are organized into layers perpendicular to the *c*-axis.

Within these layers, inversion-centered dyadic motifs are identified, which are most probably stabilized by two, almost linear, C–H···F hydrogen bonds (Figure 11). Similar C–H···F hydrogen bonds, although weak, have been shown to play a crucial role in halogenated molecules in the solid state.[25] Their geometrical characteristics [H···F = 2.508 Å, C(–H)···F = 3.430(6) Å, C–H···F = 171.5°] compare favorably with those described, for example, in *p*-difluorobenzene, whose H···F distances have been reported to be 2.49 Å,[26] as well as in several tetrathiafulvalene derivatives incorporating the very same seven-membered motif.[27]

This dyadic motif, with the $CH_2CF_2CH_2$ moiety bent away from the neighboring molecule, allows for an almost perfect eclipsed overlap between the planar C_2S_4 moieties of both complexes, although with large S···S distances of

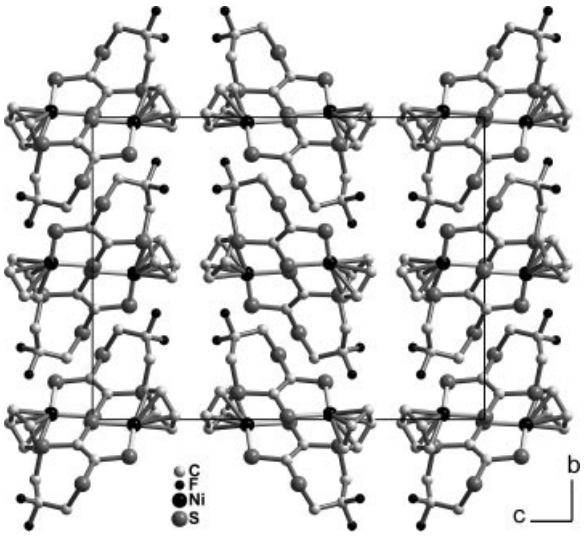

Figure 10. Projection view of the unit cell of [CpNi(CF_2)] along the *a*-axis.

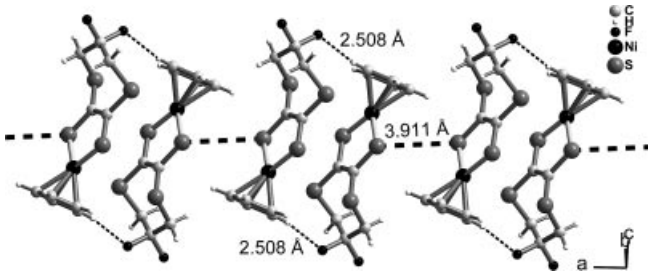

Figure 11. View of the solid-state organization of [CpNi(CF_2)] showing the C–H···F hydrogen bonds and the shortest S···S intermolecular interactions.

between 4.06 and 4.10 Å. A notably shorter S···S contact [3.911(1) Å], which furthermore involves the sulfur atoms of the metallacycles, connects these dyads together and offers a more efficient path for direct magnetic exchange interactions. The temperature dependence of the magnetic susceptibility of [CpNi(CF_2)] (Figure 12) confirms this analysis and the associated singlet–triplet behavior. Indeed, the susceptibility goes through a maximum upon cooling and decreases abruptly, as expected for a singlet ground state. It can be properly fitted to the expression $\chi = \chi_0 + (1 - \rho)\cdot 0.375/T + \rho\cdot\chi_{ST}$, where χ_0 is a temperature-independent value, $(1 - \rho)\cdot 0.375/T$ the contribution of a small fraction of Curie-type magnetic defaults, and $\rho\cdot\chi_{ST}$ the contribution of the dyads with:

$$\chi_{ST} = [(Ng^2\beta^2)/k]\cdot\{1/[3 + \exp(-J/kT)]\}$$

This affords a J_{CF_2}/k value of –11.9(1) K (8.3 cm^{-1}) with a Curie tail contribution of 3% of $S = 1/2$ magnetic defaults, thus demonstrating that at S···S distances of ca. 4 Å the overlap interaction is indeed very weak, as already noted above in the chain behavior of [CpNi(S)].

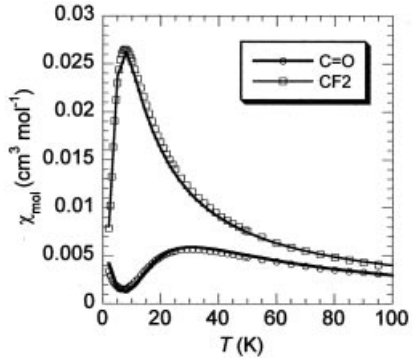

Figure 12. Temperature dependence of the magnetic susceptibility in [CpNi(C=O)] and [CpNi(CF_2)]. Solid lines are fits to the singlet–triplet model (see text).

In [CpNi(C=O)], a similar singlet–triplet behavior is observed, although with much stronger interactions since the fit of the magnetic data, performed as described above for [CpNi(CF_2)], affords a J_{CO}/k value of –50.6(4) K (35.2 cm^{-1}), together with a Curie tail contribution of 2.3% of $S = 1/2$ species.

A projection view of the unit cell of [CpNi(C=O)] is shown in Figure 13. A close observation of the solid-state organization in the structure of [CpNi(C=O)] also shows the presence of inversion-centered dyadic motifs (Figure 14), with a complex set of S···S short distances between 3.69 and 4.02 Å within columns of dyads running along the *b*-axis. Such a magnetic system is related to spin ladder systems with a singlet state as ground state, as also observed experimentally from the temperature dependence of the susceptibility. However, no analytical model is available to fit the behavior of such a complex interaction network. Therefore, the singlet–triplet fit described above can only be considered as an estimation of the strongest interaction.

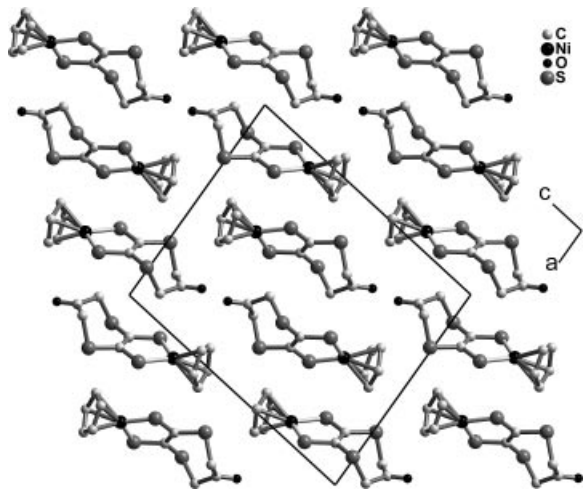

Figure 13. Projection view of the unit cell of [CpNi(C=O)].

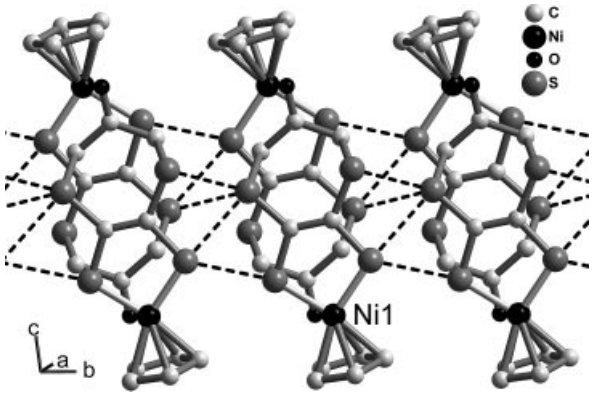

Figure 14. Shortest S···S intermolecular contacts (dotted lines) in [CpNi(C=O)].

Conclusions

The regular evolution of the electrochemical and absorption properties experimentally observed here in solution with the order $CF_2 > C=O > S > C=CH_2 > CH_2$ offers an attractive series, particularly when it comes to evaluating the origin of the NIR absorption band in these complexes. Theoretical calculations are under way to determine the nature of the transitions involved in this absorption band. The diversity of structural and magnetic behaviors encountered in this isosteric series of radical complexes demonstrates that the nature of the terminal group has a strong influence on the solid-state organization, which complements earlier observations. Indeed, while the S/Se substitution in the metallacycle was found to afford isostructural compounds as in the dithiolene/diselenolene pairs [CpNi(dmit)] vs. [CpNi(dsit)],[8a] [CpNi(dddt)] vs. [CpNi(ddds)],[8c] and [CpNi(bdt)] vs. [CpNi(bds)],[8c] a limited modification of the dithiolate ligand affecting the side heterocycle strongly modifies their crystal structure, as already observed in the following pairs, which are not isostructural: [CpNi(dmit)] vs. [CpNi(dmid)][8a] or [CpNi(dddt)] vs. [CpNi(dsdt)].[8c] More generally, the strong folding of the dithiolato ligand in the five complexes hinders the face-to-face overlap on the ligand, thus favoring one-dimensional spin chains through side-by-side interactions between sulfur atoms of the metallacycles.

Experimental Section

General Remarks: All reactions were carried out under argon by means of standard Schlenk techniques. All solvents for chemical reactions were dried and distilled from Na/benzophenone (for toluene) or CaH_2 (for methanol) before use. The square-planar (dithiolene)nickel complexes [Ni(pddt)$_2$],[10] [Ni(F_2pddt)$_2$],[11] [Ni(dpdt)$_2$],[12] and [Ni(dtdt)$_2$][13] were synthesized according to literature methods. [1,3]Dithiolo[4,5-*b*][1,4]dithiepine-2,6-dione[28] and [Cp_2Ni](BF_4)[29] were also prepared according to literature methods. [Cp_2Ni] and [CpNi(CO)]$_2$ were obtained from Strem Chemicals and Aldrich Chemicals, respectively. Silica gel (Silica gel 60) was obtained from Merck, Ltd. TOF mass spectra were recorded with a Bruker Daltonics MALDI-TOF BIFLEX III mass spectrometer. UV/Vis and NIR spectra were recorded with a Hitachi Model UV-2500PC and a Perkin Elmer Model Lambda 19 UV/Vis/NIR spectrometer, respectively. Elemental analyses were performed by the "Service d'Analyse du CNRS" at Gif/Yvette, France. UV irradiation for the photoreaction was performed with a high-pressure Hg lamp (Applied Photophysics, Ltd).

General Procedure for the Synthesis of [CpNi(CH_2)], [CpNi(CF_2)], [CpNi(C=CH_2)], and [CpNi(S)]: A toluene solution of [Cp_2Ni] (38 mg, 0.2 mmol) and the square-planar dithiolene complex [Ni(dithiolene)$_2$] (0.2 mmol) was heated at 80 °C for 2 h. After removal of the solvent under reduced pressure, the residue was extracted and separated by column chromatography (silica gel; dichloromethane/*n*-hexane, 1:1 v/v). The product was further purified by recrystallization (*n*-hexane/dichloromethane) to afford the corresponding CpNi(dithiolene) complexes: [CpNi(CH_2)] (black needles, 34.4 mg, 54% yield); [CpNi(CF_2)] (black plates, 29 mg, 41% yield); [CpNi(C=CH_2)] (black needles, 19.8 mg, 30% yield); [CpNi(S)] (dark-green blocks, 41 mg, 61% yield). Details are summarized in Table 2. In the reactions of [Ni(CH_2)$_2$] and [Ni(CF_2)$_2$] with [Cp_2Ni], the mono(dithiolene)nickel oligomers [Ni(CH_2)]$_n$ and [Ni(CF_2)]$_n$ were also obtained by column chromatography (silica gel; dichloromethane). These brown products (a few mg) were identified as hexamers (n = 6).

[CpNi(CH_2)]: TOF-MS (EI$^+$, 1.3 kV): m/z = 317 [M$^+$], 275 [M$^+$ – (CH_2)$_3$]. UV/Vis/NIR (CH_2Cl_2): λ_{max} (ε) = 848 nm (2100 $M^{-1}cm^{-1}$), 417 (5400), 329 (13000), 271 (12000). $C_{10}H_{11}NiS_4$ (318.15): calcd. C 37.75, H 3.48, S 40.32; found C 37.80, H 3.27, S 40.15.

[CpNi(CF_2)]: TOF-MS (EI$^+$, 1.3 kV): m/z = 353 [M$^+$]. UV/Vis/NIR (CH_2Cl_2): λ_{max} (ε) = 798 nm (2000 $M^{-1}cm^{-1}$), 411 (6400), 330 (15000), 264 (13000). $C_{10}H_9F_2NiS_4$ (354.13): calcd. C 33.92, H 2.56, S 36.22; found C 34.02, H 2.83, S 36.14.

[CpNi(C=CH_2)]: TOF-MS (EI$^+$, 1.3 kV): m/z = 329 [M$^+$], 301 [M$^+$ – (CH_2)$_2$], 275 [M$^+$ – (CH_2)$_2$C=CH_2]. UV/Vis/NIR (CH_2Cl_2): λ_{max} (ε) = 840 nm (2400 $M^{-1}cm^{-1}$), 419 (6500), 327 (15000), 266 (12000). $C_{11}H_{11}NiS_4$ (330.16): calcd. C 40.02, H 3.36, S 38.85; found C 40.22, H 3.65, S 38.56.

[CpNi(S)]: TOF-MS (EI$^+$, 1.3 kV): m/z = 335 [M$^+$]. UV/Vis/NIR (CH_2Cl_2): λ_{max} (ε) = 823 nm (1800 $M^{-1}cm^{-1}$), 418 (5900), 321 (14000). $C_9H_9NiS_5$ (336.19): calcd. C 32.15, H 2.70, S 47.69; found C 32.24, H 2.55, S 47.79.

Synthesis of [CpNi(C=O)]. (a) Thermal Conditions: A solution of [Cp_2Ni] (94 mg, 0.5 mmol) and [1,3]dithiolo[4,5-*b*][1,4]dithiepine-2,6-dione (118 mg, 0.5 mmol) was heated in refluxing toluene for 24 h. Silica gel was then added to the solution to oxidize remaining [Cp_2Ni] in the reaction mixture. The solvent was removed under reduced pressure, and the residue was separated by column chromatography (silica gel; dichloromethane/*n*-hexane, 1:1 v/v) to afford [CpNi(C=O)] as a black solid (15 mg, 9% yield). The same reaction performed with 2 equiv. of [1,3]dithiolo[4,5-*b*][1,4]dithiepine-2,6-dione and a shorter reaction time (6 h) afforded 25 mg of [CpNi(C=O)] in a slightly improved 15% yield. **(b) Photochemical Conditions:** A toluene solution (300 mL) of [Cp_2Ni] (57 mg, 0.3 mmol, $c = 1.0 \times 10^{-3}$ M) and [1,3]dithiolo[4,5-*b*][1,4]dithiepine-2,6-dione (71 mg, 0.3 mmol, $c = 1.0 \times 10^{-3}$ M) was irradiated with a high-pressure Hg lamp (400 W) for 24 h. A black precipitate was filtered off, and the solvent removed under reduced pressure. The reaction mixture was separated by column chromatography (silica gel; dichloromethane/*n*-hexane, 1:1 v/v) to afford [CpNi(C=O)] as a black solid (15 mg, 9% yield).

[CpNi(C=O)]: TOF-MS (EI$^+$, 1.3 kV): m/z = 331 [M$^+$], 275 [M$^+$ – (CH_2)$_2$C=O]. UV/Vis/NIR (CH_2Cl_2): λ_{max} (ε) = 806 nm (1700 $M^{-1}cm^{-1}$), 416 (5600), 325 (13000), 264 (11000). $C_{10}H_9NiOS_4$

Table 6. Crystallographic data of CpNi(dithiolene) complexes.[a]

	[CpNi(CH_2)]	[CpNi(CF_2)]	[CpNi(C=CH_2)]	[CpNi(S)]	[CpNi(C=O)]
Empirical formula	$C_{10}H_{11}NiS_4$	$C_{10}H_9F_2NiS_4$	$C_{11}H_{11}NiS_4$	$C_9H_9NiS_5$	$C_{10}H_9NiOS_4$
Formula mass [g mol^{-1}]	318.14	354.12	330.15	336.17	332.12
Crystal system	triclinic	orthorhomic	monoclinic	monoclinic	monoclinic
Space group	$P\bar{1}$ (no. 2)	*Pbca* (no. 61)	$P2_1$ (no. 4)	$P2_1/c$ (no. 14)	$P2_1/n$ (no. 14)
a [Å]	5.5452(8)	9.3407(9)	5.6953(11)	10.9076(10)	12.8566(15)
b [Å]	9.9075(15)	14.8645(12)	11.1493(16)	6.1650(4)	6.1488(5)
c [Å]	11.4352(16)	19.2204(15)	10.484(2)	18.5748(16)	15.4174(17)
α [°]	89.756(18)	–	–	–	–
β [°]	85.714(17)	–	99.54(2)	97.731(11)	97.012(14)
γ [°]	86.397(18)	–	–	–	–
V [Å^3]	625.24(16)	2668.7(4)	656.5(2)	1237.72(18)	1209.7(2)
T [K]	293(2)	293(2)	293(2)	293(2)	293(2)
Z	2	8	2	4	4
$D_{calcd.}$ [g cm^{-3}]	1.690	1.763	1.670	1.804	1.824
μ [mm^{-1}]	2.182	2.075	2.081	2.372	2.270
Total reflections	6053	22010	6450	9122	8817
Absorption correction	multi-scan	gaussian	multi-scan	multi-scan	gaussian
Independent reflections (R_{int})	2239 (0.0395)	2581 (0.0772)	2526 (0.0475)	2351 (0.0313)	2260 (0.0471)
Reflections [$I > 2\sigma(I)$]	1872	1690	1646	1794	1503
R_1, wR_2 [$I > 2\sigma(I)$]	0.0343, 0.0918	0.0306, 0.0540	0.0277, 0.0445	0.0275, 0.0694	0.0270, 0.0455
R_1, wR_2 (all data)	0.0442, 0.0969	0.0631, 0.0608	0.0594, 0.0498	0.0396, 0.0756	0.0568, 0.0501
Goodness-of-fit	1.055	0.882	0.845	0.737	0.849

[a] $R_1 = \Sigma||F_o| - |F_c||/\Sigma|F_o|$; $wR_2 = [\Sigma w(F_o^2 - F_c^2)^2/\Sigma wF_o^4]^{1/2}$.

(332.13): calcd. C 36.16, H 2.73, S 38.62; found C 35.98, H 2.65, S 38.43.

CV Measurements: All electrochemical measurements were performed under argon. Solvents for electrochemical measurements were dried over molecular sieves (4 Å) before use. A platinum wire served as a counter electrode, and the reference electrode (Ag/AgCl) was corrected for junction potentials by being referenced internally to the ferrocene/ferrocenium (Fc/Fc^+) couple. A stationary platinum disk (1.6 mm in diameter) was used as working electrode. A Model CV-50W instrument from BAS Co. was used for cyclic voltammetry (CV) measurements. CVs were measured in 1 mM dichloromethane solutions of complexes containing 0.1 M tetrabutylammonium hexafluorophosphate (Bu_4NPF_6) at 25 °C.

EPR Measurements: EPR spectra were recorded with a Bruker ESP 300 spectrometer (X-band) equipped with a variable-temperature attachment from 1 mM dichloromethane solutions of complexes. Optimizations and simulations of the frozen solution spectra were carried out with a program, based on the Levenberg–Marquardt least-squares fit, which compares the position of the experimental resonance lines with those calculated by second-order perturbation theory.

X-ray Diffraction Studies: Single crystals of [CpNi(dithiolene)] complexes were obtained by recrystallization from dichloromethane solution and then vapor diffusion of *n*-hexane into these solutions. A crystal was mounted on the top of a thin glass fiber. Data were collected with a Stoe Imaging Plate Diffraction System (IPDS) with graphite-monochromated Mo-K_α radiation (λ = 0.71073 Å) at room temperature. Structures were solved by direct methods (SHELXS-97) and refined (SHELXL-97)[30] by full-matrix least-squares methods, as implemented in the WinGX software package.[31] Absorption corrections were applied. Hydrogen atoms were introduced at calculated positions (riding model), included in structure factor calculations, and not refined. Crystallographic data of complexes are summarized in Table 6. CCDC-614018 {[CpNi(C=CH_2)]}, -614019 {[CpNi(CF_2)}, -614020 {[CpNi(CH_2)]}, -614021 {[CpNi(C=O)]} and -614022 {[CpNi(S)]} contain the supplementary crystallographic data for this paper. These data can be obtained free of charge from The Cambridge Crystallographic Data Centre via www.ccdc.cam.ac.uk/data_request/cif.

Acknowledgments

We thank Prof. Masatsugu Kajitani (Sophia University) for his help with the CV measurements. We also thank the Ministère de la Recherche (France) for a postdoctoral grant (to M. N.) and the CNRS (France) and the National Swiss Foundation for financial support.

[1] a) S. D. Cummings, R. Eisenberg, *Prog. Inorg. Chem.* **2003**, *52*, 315; b) H. Kisch, *Coord. Chem. Rev.* **1993**, *125*, 155.
[2] a) A. T. Coomber, D. Beljonne, R. H. Friend, J. L. Bredas, A. Charlton, N. Robertson, A. E. Underhill, M. Kurmoo, P. Day, *Nature* **1996**, *380*, 144; b) C. Faulmann, P. Cassoux, *Prog. Inorg. Chem.* **2003**, *52*, 399.
[3] a) P. Cassoux, L. Valade, H. Kobayashi, A. Kobayashi, R. A. Clark, A. E. Underhill, *Coord. Chem. Rev.* **1991**, *110*, 115; b) R.-M. Olk, B. Olk, W. Dietzsch, R. Kirmse, E. Hoyer, *Coord. Chem. Rev.* **1992**, *117*, 99; c) R. Kato, *Chem. Rev.* **2004**, *104*, 5319; d) G. Matsubayashi, M. Nakano, H. Tamura, *Coord. Chem. Rev.* **2002**, *226*, 143.
[4] a) C. L. Beswick, J. M. Schulman, E. I. Stiefel, *Prog. Inorg. Chem.* **2003**, *52*, 55; b) G. N. Schrauzer, *Acc. Chem. Res.* **1969**, *2*, 72 and references cited therein.
[5] a) W. Paw, S. D. Cummings, M. A. Mansour, W. B. Connick, B. K. Geiger, R. Eisenberg, *Coord. Chem. Rev.* **1998**, *171*, 125; b) J. A. Zuleta, J. M. Bevilacqua, R. Eisenberg, *Coord. Chem. Rev.* **1991**, *111*, 237; c) J. A. Zuleta, M. S. Burberry, R. Eisenberg, *Coord. Chem. Rev.* **1990**, *97*, 47.
[6] M. Fourmigué, *Coord. Chem. Rev.* **1998**, *178*, 823 and references cited therein.
[7] M. Fourmigué, *Acc. Chem. Res.* **2004**, *37*, 179.
[8] a) M. Fourmigué, N. Avarvari, *Dalton Trans.* **2005**, 1365; b) M. Nomura, R. Okuyama, C. Fujita-Takayama, M. Kajitani, *Organometallics* **2005**, *24*, 5110; c) M. Nomura, T. Cauchy, M. Geoffroy, P. Adkine, M. Fourmigué, *Inorg. Chem.* **2006**, *45*, 8194.

[9] C. Faulmann, F. Delpech, I. Malfant, P. Cassoux, *J. Chem. Soc., Dalton Trans.* **1996**, 2261.
[10] a) R. D. Bereman, H. Lu, *Inorg. Chim. Acta* **1993**, *204*, 53; b) U. Geiser, S. F. Tytko, T. J. Allen, H. H. Wang, A. M. Kini, J. M. Williams, *Acta Crystallogr., Sect. C* **1991**, *47*, 1164.
[11] a) O. J. Dautel, M. Fourmigué, *Inorg. Chem.* **2001**, *40*, 2083; b) O. J. Dautel, M. Fourmigué, E. Canadell, P. Auban-Senzier, *Adv. Funct. Mater.* **2002**, *12*, 693.
[12] a) A. Charlton, A. E. Underhill, A. Kobayashi, H. Kobayashi, *J. Chem. Soc., Dalton Trans.* **1995**, 1285; b) A. Charlton, A. E. Underhill, K. M. A. Malik, M. B. Hursthouse, T. Jørgensen, J. Becher, *Synth. Met.* **1995**, *68*, 221.
[13] a) R. Kato, H. Kobayashi, A. Kobayashi, Y. Sasaka, *Bull. Chem. Soc. Jpn.* **1986**, *59*, 627; b) C. Faulmann, A. Errami, B. Donnadieu, I. Malfant, J.-P. Legros, P. Cassoux, C. Rovira, E. Canadell, *Inorg. Chem.* **1996**, *35*, 3856.
[14] R. B. King, *J. Am. Chem. Soc.* **1963**, *85*, 1587.
[15] a) W. Kusters, P. De Mayo, *J. Am. Chem. Soc.* **1974**, *96*, 3502; b) W. Schroth, H. Bahn, R. Zschernitz, *Z. Chem.* **1973**, *13*, 424; c) R. Schulz, A. Schweig, K. Hartke, J. Koester, *J. Am. Chem. Soc.* **1983**, *105*, 4519.
[16] TOF MS (no matrix): *m/z* = 1518 $[Ni\{S_2C_2S_2(CH_2)_3\}]_6$ $[M^+]$ and 1734 $[Ni\{S_2C_2S_2(CH_2)_2(CF_2)\}]_6$ $[M^+]$.
[17] T. B. Rauchfuss, *Prog. Inorg. Chem.* **2003**, *52*, 1.
[18] R. E. Dessy, F. E. Stary, R. B. King, M. Waldrop, *J. Am. Chem. Soc.* **1966**, *88*, 471.
[19] J. A. McCleverty, T. A. James, E. J. Wharton, *Inorg. Chem.* **1969**, *8*, 1340.
[20] a) C. Takayama, M. Kajitani, T. Sugiyama, A. Sugimori, *J. Organomet. Chem.* **1998**, *563*, 161; b) M. Fourmigué, V. Perrocheau, *Acta Crystallogr., Sect. C* **1997**, *53*, 1213.
[21] K. Kawabata, M. Nakano, H. Tamura, G. Matsubayashi, *J. Organomet. Chem.* **2004**, *689*, 405.
[22] G.-X. Jin, M. Herberhold, A. L. Rheingold, *New J. Chem.* **1998**, *22*, 1035.
[23] a) K. Mashima, H. Kaneyoshi, S. Kaneko, A. Mikami, K. Tani, A. Nakamura, *Organometallics* **1997**, *16*, 1016; b) M. Nomura, M. Fujii, K. Fukuda, T. Sugiyama, Y. Yokoyama, M. Kajitani, *J. Organomet. Chem.* **2005**, *690*, 1627.
[24] O. Kahn, *Molecular Magnetism*, VCH, Weinheim, **1993**, chapter 11.
[25] G. R. Desiraju, T. Steiner, in *The Weak Hydrogen Bond*, Oxford University Press, New York, **1999**.
[26] V. R. Thalladi, H.-C. Weiss, D. Bläser, R. Boese, A. Nangia, G. R. Desiraju, *J. Am. Chem. Soc.* **1998**, *120*, 8702.
[27] a) O. J. Dautel, M. Fourmigué, *J. Org. Chem.* **2000**, *65*, 6479; b) O. J. Dautel, M. Fourmigué, E. Canadell, *Chem. Eur. J.* **2001**, *7*, 2635.
[28] M. R. Bryce, G. J. Marshallsay, *Tetrahedron Lett.* **1991**, *32*, 6033.
[29] J. S. Miller, J. C. Calabrese, H. Rommelmann, S. R. Chittipeddi, J. H. Zhang, W. M. Reiff, A. J. Epstein, *J. Am. Chem. Soc.* **1987**, *109*, 769.
[30] SHELX97, Program for Crystal Structure Analysis (release 97-2). G. M. Sheldrick, **1998**.
[31] L. J. Farrugia, *J. Appl. Crystallogr.* **1999**, *32*, 837.

Received: July 11, 2006
Published Online: October 31, 2006

